

Three-Dimensional Mathematical Model for Deformation of Human Fasciae in Manual Therapy

Hans Chaudhry, PhD; Robert Schleip, MA; Zhiming Ji, PhD; Bruce Bukiet, PhD; Miriam Maney, MS; and Thomas Findley, MD, PhD

Context: Although mathematical models have been developed for the bony movement occurring during chiropractic manipulation, such models are not available for soft tissue motion.

Objective: To develop a three-dimensional mathematical model for exploring the relationship between mechanical forces and deformation of human fasciae in manual therapy using a finite deformation theory.

Methods: The predicted stresses required to produce plastic deformation were evaluated for a volunteer subject's fascia lata, plantar fascia, and superficial nasal fascia. These stresses were then compared with previous experimental findings for plastic deformation in dense connective tissues. Using the three-dimensional mathematical model, the authors determined the changing amounts of compression and shear produced in fascial tissue during 20 seconds of manual therapy.

Results: The three-dimensional model's equations revealed that very large forces, outside the normal physiologic range, are required to produce even 1% compression and 1% shear in fascia lata and plantar fascia. Such large forces are not required to produce substantial compression and shear in superficial nasal fascia, however.

Conclusion: The palpable sensations of tissue release that are often reported by osteopathic physicians and other manual therapists cannot be due to deformations produced in the firm tissues of plantar fascia and fascia lata. However, palpable tissue release could result from deformation in softer tissues, such as superficial nasal fascia.

J Am Osteopath Assoc. 2008;108:379-390

From the departments of Biomedical Engineering (Drs Chaudhry and Findley), Mechanical Engineering (Dr Ji), and Mathematical Sciences (Dr Bukiet) at the New Jersey Institute of Technology in Newark; the Department of Applied Physiology at Ulm University in Germany (Mr Schleip); and the War-Related Illness and Injury Study Center at the Veterans Affairs Medical Center in East Orange, NJ (Drs Chaudhry and Findley, Ms Maney).

This study was partially supported by a dissertation grant from the International Society of Biomechanics to Mr Schleip's Fascia Research Project.

Address correspondence to Zhiming Ji, PhD, Department of Mechanical Engineering, New Jersey Institute of Technology, Newark, NJ 07102-1982.

E-mail: ji@njit.edu

Submitted March 23, 2006; revision received June 20, 2006; accepted August 10, 2006.

Fascia is dense fibrous connective tissue that connects muscles, bones, and organs, forming a continuous network of tissue throughout the body. It plays an important role in transmitting mechanical forces during changes in human posture. Several forms of manual fascial therapies—including myofascial release and certain other techniques in osteopathic manipulative treatment (OMT)—have been developed to improve postural alignment and other expressions of musculoskeletal dynamics.^{1,2} The purpose of these therapies and treatments is to alter the mechanical properties of fascia, such as density, stiffness, and viscosity, so that the fascia can more readily adapt to physical stresses.^{3,4} In fact, some osteopathic physicians and manual therapists report local tissue release after the application of a slow manual force to tight fascial areas.^{2,4,5} These reports have been explained as a breaking of fascial cross-links, a transition from gel to sol state in the extracellular matrix, and other passive viscoelastic changes of fasciae.^{2,4,5}

The question of whether the applied force and duration of a given manual technique (eg, myofascial) could be sufficient to induce palpable viscoelastic changes in human fasciae is unresolved, with some authors^{1,5,6} supporting the likelihood of such an effect and others^{7,8} arguing against it.

Our intent in undertaking the present study was to resolve this question. Therefore, we present an original mathematical model to determine if forces applied in manual therapy are sufficient to produce tissue deformation in human fasciae.

Background

The mechanical properties of ex vivo rat superficial fascia (ie, subcutaneous tissue) under uniaxial tension have been reported by Iatridis et al,⁹ who investigated the potential importance of uniaxial tension in a variety of therapies involving mechanical stretch. The mechanical properties of in vitro human superficial nasal fascia and nasal periosteum were investigated by Zeng et al¹⁰ to determine under which tissue layer silicon implants should be inserted for improved results in aesthetic surgical corrections of congenital saddle nose and flat nose. Similarly, the mechanical properties of in vitro fascia lata and plantar fascia have been investigated by Wright and Rennels.¹¹ The results of each of these studies of fascial mechanical properties can be used in determining the types and strengths of mechanical forces needed to produce desired deformations during manual therapy.

ORIGINAL CONTRIBUTION

In recommending further study of manual therapies, Threlkeld⁷ noted that the three-dimensional dispersion of forces in relatively intact regions of the human body had yet to be investigated. Although mathematical models have since been developed for the bony movement resulting from applied forces in chiropractic high-velocity manipulations with human subjects,¹²⁻¹⁵ no such attempts have yet been made—to our knowledge—for other manual therapies, including OMT.

This lack of a mathematical model motivated us to model the relationship between mechanical forces and deformation of human fasciae during manual therapy. We believe that this new mathematical model may be useful in future calculations of the forces required to induce desired plastic tissue deformations in a manual therapeutic context, including in such osteopathic manipulative procedures as soft tissue techniques and fascial-ligamentous release.

Methods

Because fasciae are known to experience finite strain,¹⁰ we used a finite deformation theory of elasticity¹⁶ to develop our three-dimensional model for exploring the relationship between mechanical forces applied on the surfaces of human fascia in manual therapy and the resulting deformation of the fascia. In continuum mechanics, finite deformation theory is used when the deformation of a body is sufficiently large to overcome the assumptions inherent in small strain theory.¹⁶ This is commonly the case with elastomers and other fluids and biological soft tissue.¹⁶

We then applied this model to manual therapy in a laboratory setting to evaluate the mechanical forces needed to produce specific types of deformation in fascia lata, plantar fascia, and superficial nasal fascia. We used previously reported longitudinal stress-strain data^{10,11} in the application of our model.

The inclusion of superficial nasal fascia, which is much softer tissue than fascia lata and plantar fascia, allowed us to test whether our model equations could predict significant compression and shear in pliable tissue compared with stiff tissue. The present study was conducted with the approval of the Institutional Review Board at the Veterans Affairs Medical Center in East Orange, NJ.

New Mathematical Model

Our three-dimensional model (*Figure 1*) allowed us to determine the mechanical forces applied on the surfaces of fascia that result in particular types of deformation. Because of the lack of more specific data on the structure of superficial nasal fascia and its mechanical properties, we assumed for the purpose of this first mathematical model that this fascia was isotropic. We also followed the assumption that fascia lata, plantar fascia, and superficial nasal fascia are composed of incompressible material,¹⁰ as are most soft biological tissues.

The basic kinematics and kinetics equations used to evaluate the stresses under specified deformations are presented

below and in subsequent pages in equations (1-4, 10, 12, 13).¹⁶ The stress results from these equations were required to satisfy differential equations of equilibrium and boundary conditions, which in turn allowed us to determine the mechanical forces needed to produce the specified deformations.

The metric tensors g_{ij} and g^{ij} in the Cartesian coordinates x^i ($i = 1, 2, 3$) in the undeformed state are given by the following:

$$(1) \quad g_{ij} = \frac{\partial x^r}{\partial x^i} \frac{\partial x^r}{\partial x^j}, \quad g^{ij} = \frac{\partial x^i}{\partial x^r} \frac{\partial x^j}{\partial x^r}, \quad (r = 1, 2, 3; \quad i, j = 1, 2, 3)$$

The repeated index, r , in equation (1) means summation over r .

Similarly, the metric tensors G_{ij} and G^{ij} in the deformed-state Cartesian coordinates y^r ($r = 1, 2, 3$) are given by the following:

$$(2) \quad G_{ij} = \frac{\partial y^r}{\partial y^i} \frac{\partial y^r}{\partial y^j}, \quad G^{ij} = \frac{\partial y^i}{\partial y^r} \frac{\partial y^j}{\partial y^r}, \quad (r = 1, 2, 3; \quad i, j = 1, 2, 3)$$

From equation (1), we find that:

$$(3) \quad g_{ij} = g^{ij} = \delta_{ij} \text{ (Kronecker delta)}, \quad g = |g_{ij}|$$

In equation (3), $|g_{ij}|$ is the determinant of the matrix g_{ij} . Thus, $g = 1$.

The metric tensors defined in the equations presented above are the measures of fascial deformation in three dimensions—when the fascia are subjected to normal, longitudinal, and tangential forces. The physical meaning of these tensors can be understood by their relation to the strain E^{ij} in the following equation:

$$(4) \quad E^{ij} = \frac{G^{ij} - g^{ij}}{2}$$

■ **Deformation of Fasciae**—We assumed the manipulation-caused fascial deformations of shear and elongation along the x^1 -axis, extension along the x^2 -axis, and compression along the negative x^3 -axis (*Figure 1*) to be given by the following:

$$(5) \quad y^1 = x^1 + k_1 x^3 + k_4 x^1, \quad y^2 = k_2 x^2, \quad y^3 = k_3 x^3, \\ (k_3 < 1, \quad k_1, \quad k_2, \quad k_4 > 0)$$

In equation (5), the y^i -axes in the deformed state of the fascia coincide with the x^i -axes in the undeformed state of the fascia.

Also in equation (5), k_1 denotes the shear ratio due to the application of the tangential force. The maximum shear occurs at the surface of the fascia, where the fascial thickness is at its maximum. The shear is zero at the bottom of the fascia, where fascial thickness is zero. In addition, k_4 is the extension ratio due to the applied longitudinal force, k_3 denotes the compression

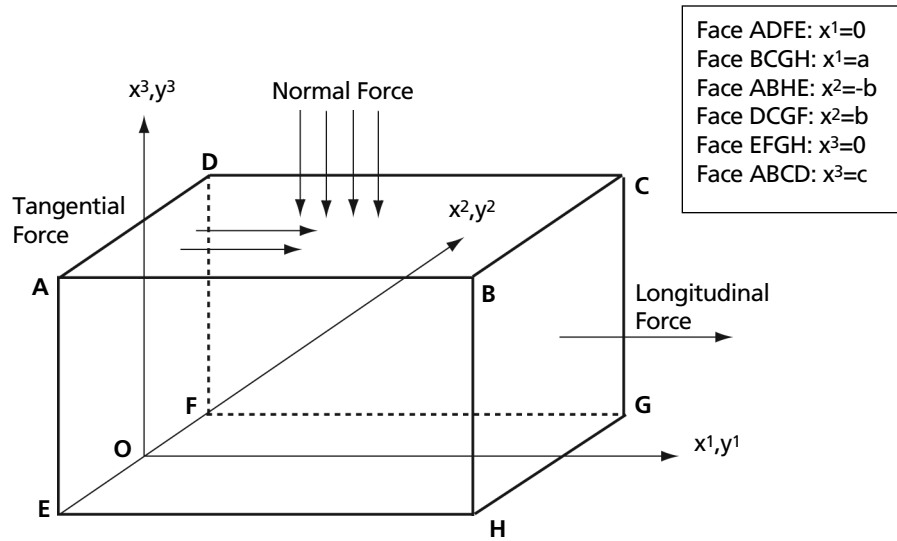


Figure 1. Three-dimensional model of fascial element subjected to normal, tangential, and longitudinal forces in the undeformed state. The axes (x^1, x^2, x^3) in the undeformed state coincide with the axes (y^1, y^2, y^3) in the deformed state. The six faces of this modeled fascial element are designated with capital letters. The symbols $a, b,$ and c represent the coordinate values of the faces along the $x^1, x^2,$ and x^3 axes.

y^2, y^3) in the deformed state. The six faces of this modeled fascial element are designated with capital letters. The symbols $a, b,$ and c represent the coordinate values of the faces along the $x^1, x^2,$ and x^3 axes.

ratio due to the applied normal pressure, and k_2 is the extension ratio resulting from the compression caused by manual therapy on the surface of the fascia.

Typically, in OMT and other forms of manual therapy, compression and shear are applied to most fasciae. However, in some cases, such as with fascia lata, extension is also applied, such as by bending the lower leg at the knee. It should be noted that smaller values of k_3 mean more compression. For example, $k_3 = 0.90$ means 10% compression. The values for k_2 can be determined in terms of k_3 and k_4 using the incompressibility condition described in equations (9) through (11).

Thus, using equations (2) and (5), we get the following (in which zero represents the value of the corresponding tensor elements):

$$(6) \quad G_{ij} = \begin{bmatrix} (1+k_4)^2 & 0 & k_1(1+k_4) \\ 0 & k_2^2 & 0 \\ k_1(1+k_4) & 0 & k_1^2+k_3^2 \end{bmatrix}$$

$$(7) \quad G^{ij} = \begin{bmatrix} \frac{(k_3^2+k_1^2)}{k_3^2(1+k_4)^2} & 0 & \frac{-k_1}{k_3^2(1+k_4)} \\ 0 & \frac{1}{k_2^2} & 0 \\ \frac{-k_1}{(1+k_4)k_3^2} & 0 & \frac{1}{k_3^2} \end{bmatrix}$$

The strain invariants $I_1, I_2,$ and I_3 (which are needed to evaluate stresses) are given by the following:

$$(8) \quad I_1 = g^{rs}G_{rs}, \quad I_2 = g_{rs}G^{rs}, \quad I_3 = \frac{G}{g}$$

In equation (8), G is the determinant of the matrix G_{ij} , while G from equation (6) is: $k_2^2 [(1+k_4)^2 k_3^2]$. The invariants in equation (8) are invariants in strain that do not change with the coordinate system.

Using equations (3) and (6) through (8), we get the following:

$$(9) \quad I_1 = k_1^2 + k_3^2 + k_2^2 + (1+k_4)^2; \quad I_2 = \frac{(k_3^2+k_1^2)}{(1+k_4)^2 k_3^2} + \frac{1}{k_2^2} + \frac{1}{k_3^2};$$

$$I_3 = \frac{G}{g} = k_2^2 [(1+k_4)^2 k_3^2]$$

Because the fasciae are assumed to be incompressible, we have:

$$I_3 = 1, \quad \text{thus, } k_2 = \frac{1}{k_3(1+k_4)}$$

To determine the tensor B^{ij} (which is needed to evaluate stresses), we can use the following equation:

$$(10) \quad B^{ij} = I_1 g^{ij} - g^{ir} g^{js} G_{rs}$$

ORIGINAL CONTRIBUTION

Therefore, using equations (3), (7), and (10), we obtain:

$$(11) B^{ij} = \begin{bmatrix} k_1^2 + k_2^2 + k_3^2 & 0 & -k_1(1 + k_4) \\ 0 & k_1^2 + k_3^2 + (1 + k_4)^2 & 0 \\ -k_1(1 + k_4) & 0 & k_2^2 + (1 + k_4)^2 \end{bmatrix}$$

■ **Stress Evaluation**—The stresses placed on fascia can be evaluated by using the following equation¹³:

$$(12) \tau^{ij} = \varphi g^{ij} + \psi B^{ij} + p G^{ij}$$

In equation (12), we note the following:

$$(13) \varphi = 2 \frac{\partial W}{\partial I_1}, \psi = 2 \frac{\partial W}{\partial I_2}, p = 2 \frac{\partial W}{\partial I_3}$$

In equation (13), W is the strain energy function.

In our mathematical model, we used the form of the strain energy function for isotropic soft tissues described by Demiray.¹⁷ This function is given by:

$$(14) W = C_1 [e^{C_2(I_1-3)} - 1]$$

In equation (14), C_1 and C_2 are mechanical parameters to be determined, with C_1 analogous to the modulus of elasticity and C_2 a dimensionless constant. These parameters are both analogous to the elastic parameters in the small deformation theory of elasticity.¹⁶ The values of these parameters can be determined by curve fitting, as explained in “Estimation of Mechanical Constants” on page 383. In equation (14), $e = 2.71828$, which is the base of an exponential function.

Using equations (3), (5), (11), and (12), we find that the stresses are given by the following set of equations (with the superscripts after τ representing indices in the tensor notation):

$$(15) \begin{aligned} \tau^{11} &= \varphi + \psi (k_1^2 + k_2^2 + k_3^2) + p \left[\frac{(k_3^2 + k_1^2)}{k_3^2 (1 + k_4)^2} \right] \\ \tau^{22} &= \varphi + \psi \left[k_1^2 + k_3^2 + (1 + k_4)^2 \right] + p \left(\frac{1}{k_2^2} \right) \\ \tau^{33} &= \varphi + \psi \left[k_2^2 + (1 + k_4)^2 \right] + \frac{p}{k_3^2} \\ \tau^{12} &= \tau^{21} = 0 \\ \tau^{23} &= \tau^{32} = 0 \\ \tau^{13} &= \tau^{31} = -[k_1(1 + k_4)\psi] - \frac{pk_1}{k_3^2(1 + k_4)} \end{aligned}$$

In these equations, p is a scalar invariant denoting the pressure used for incompressibility constraint.

■ **Equations of Equilibrium**—It should be noted that all of the stresses in our mathematical model are constants. Therefore, the equations of equilibrium in Cartesian coordinates are satisfied because p is a constant in the following:

$$\frac{\partial p}{\partial y_1} = \frac{\partial p}{\partial y_2} = \frac{\partial p}{\partial y_3} = 0$$

To determine the value of p , we used our model to make the normal stress (τ^{33}) vanish when there is no deformation (ie, when $k_1 = k_4 = 0$ and $k_3 = k_2 = 1$). Then, we find that $p = -(\varphi + 2\psi)$. Substituting this value of p in the equations for other stresses in (15), the stresses then reduce to the following:

$$(16) \begin{aligned} \tau^{11} &= \varphi \left[1 - \frac{k_3^2 + k_1^2}{k_3^2 (1 + k_4)^2} \right] + \psi \left[k_1^2 + k_2^2 + k_3^2 - 2 \frac{(k_3^2 + k_1^2)}{k_3^2 (1 + k_4)^2} \right] \\ \tau^{22} &= \varphi \left(1 - \frac{1}{k_2^2} \right) + \psi \left[k_1^2 + k_3^2 + (1 + k_4)^2 - \frac{2}{k_2^2} \right] \\ \tau^{33} &= \varphi \left(1 - \frac{1}{k_3^2} \right) + \psi \left[(1 + k_4)^2 + k_2^2 - \frac{2}{k_3^2} \right] \\ \tau^{13} &= \tau^{31} = \varphi \left[\frac{k_1}{k_3^2(1 + k_4)} \right] + \psi \left[\frac{2k_1}{k_3^2(1 + k_4)} - k_1(1 + k_4) \right] \\ \tau^{12} &= \tau^{21} = \tau^{23} = \tau^{32} = 0 \end{aligned}$$

For the stresses in equation (16), the following should be noted:

$$k_2 = \frac{1}{k_3(1 + k_4)}$$

■ **Boundary Conditions (Formulae for Applied Forces)**—We next determined the surface forces placed by manual therapy on the fascial faces that were initially located (ie, located before deformation) at $x^1 = a$, $x^2 = b$, and $x^3 = c$ (Figure 1). All the fascial faces become curved in the deformed state during manual therapy, so the directions of the unit normal to these faces (ie, the vectors perpendicular to the faces) change.

For the face that was initially located at $x^1 = a$, the unit normal vector $\vec{\eta}$ in the deformed state is given by the following:

$$\vec{\eta} = \frac{\vec{G}^1}{\sqrt{G^{11}}}$$

In the above equation, \vec{G}^1 is the contravariant base vector.

Using equation (8), we get the following:

$$n_1 = \frac{k_3(1 + k_4)}{\sqrt{k_3^2 + k_1^2}}, n_2 = 0, n_3 = 0$$

In the above equation, $n_1, n_2,$ and n_3 are the normal components of the unit normal vector.

The force on the face $x^1 = a$ is given by the following¹⁶:

$$\vec{P} = P^k \vec{G}_k = \tau^{ik} n_i \vec{G}_k$$

The component of this force along $B'C'$, which was initially BC (Figure 1), becomes:

$$\vec{P} \cdot \frac{\vec{G}_2}{\sqrt{G_{22}}}$$

Using the above equation together with equations (6) and (16), we find that the force along $B'C'$ becomes 0. Along the line that was initially BH (Figure 1), the force is given by:

$$\vec{P} \cdot \frac{\vec{G}_3}{\sqrt{G_{33}}}$$

Using this equation with equations (6) and (16), we find that the force along $B'H'$, which was initially BH , is given by the following:

$$(17) \frac{k_3(1 + k_4)}{k_3^2 + k_1^2} [k_1(1 + k_4)\tau^{11} + \tau^{13}(k_1^2 + k_3^2)]$$

The force along the normal direction on the $x^1 = a$ face is given by the following:

$$(18) \vec{P} \cdot \frac{\vec{G}^1}{\sqrt{G^{11}}} = \frac{k_3^2(1 + k_4)^2}{k_3^2 + k_1^2} (\tau^{11}) = \frac{k_3^2(1 + k_4)^2}{k_3^2 + k_1^2}$$

$$\left[\varphi \left(1 - \frac{k_3^2 + k_1^2}{k_3^2(1 + k_4^2)} \right) + \psi \left(k_1^2 + k_2^2 + k_3^2 - 2 \frac{k_3^2 + k_1^2}{k_3^2(1 + k_4^2)} \right) \right]$$

The forces in the above equations (17) and (18) are shown as per unit area of the deformed fascial surface. In addition, the forces given by equation (17) are provided by the tissues adjacent to the fascial face $x^1 = a$.

Using the mathematical procedure described above for the fascial faces that were initially located at $x^2 = b$ and $x^3 = c$ (Figure 1), we find that on the face $x^2 = b$, the shear force vanishes but the normal force does not. The normal force on this face is given by $k_2^2\tau^{22}$. This force must be provided by the adjacent tissues because no external force is applied on this face.

On the face that was initially located at $x^3 = c$ (Figure 1), the applied normal force (N) can be evaluated as the following:

$$(19) N = k_3^2\tau^{33} = (k_3^2 - 1)\varphi + \psi[k_2^2k_3^2 + (1 + k_4)^2k_3^2 - 2]$$

Because $k_3 < 1$, the force in equation (19) is compressive, as would be expected. The applied tangential force (T) along $B'C'$ is zero throughout the duration of manual therapy, whereas the applied tangential force along $C'D'$, which is initially CD (Figure 1), on the $x^3 = c$ face can be evaluated as:

$$(20) T = \frac{k_3}{1 + k_4} [\tau^{31}(1 + k_4)^2 + \tau^{33}(1 + k_4)k_1] = k_1k_3\varphi + k_1k_3k_2^2\psi$$

The applied normal and tangential forces, as well as the extension force, must vanish if there is no shear, extension, and compression (ie, $k_1 = k_4 = 0$ and $k_3 = 1$). Equations (19) and (20) confirm this assumption.

Using equations (13) and (14), we arrive at the following:

$$(21) \varphi = 2C_1C_2e^{C_2(l_1-3)} \text{ and } \psi = 0$$

Thus, by using equations (19) and (21), the normal pressure (N) is reduced according to:

$$(22) N = 2(k_3^2 - 1)C_1C_2e^{C_2(l_1-3)}$$

From equations (20) and (21), we see that the tangential force (T) along CD becomes:

$$(23) T = 2k_1k_3C_1C_2e^{C_2(l_1-3)}$$

Using equation (18), the extension force (F) becomes:

$$(24) F = 2C_1C_2e^{C_2(l_1-3)} \left[\frac{k_3^2(1 + k_4)^2}{k_3^2 + k_1^2} - 1 \right]$$

Equations (22) through (24) are the formulae for determining the applied forces (ie, normal, tangential, and extension) during manual therapy (Figure 1). Using specified values of k_1 through k_4 and the mechanical constants (C_1 and C_2), we can determine the applied forces (N , T , and F) from the above equations of our mathematical model. Conversely, if the values of applied forces are known, we can use the equations to determine the values of k_1 through k_4 .

Estimation of Mechanical Constants

In estimating the mechanical constants, C_1 and C_2 , for fasciae in the above formulae for applied forces, we first determined the constants for the superficial nasal fascia. We used the available experimentally obtained in vitro finite stress-strain data¹⁰ for superficial nasal fascia along the longitudinal direction. This longitudinal stress is given by the following:

$$(25) \sigma = \alpha E^\beta$$

ORIGINAL CONTRIBUTION

In equation (25), σ is the longitudinal Euler's stress, and E is the Green's strain tensor.¹⁸ Green's strain tensor is the strain tensor referring to the undeformed coordinates, whereas Euler's strain tensor refers to deformed coordinates. The stress corresponding to Euler's strain is Euler's stress.¹⁸ Green's strain tensor can be calculated by the following:

$$(26) E = \frac{1}{2} (\lambda^2 - 1)$$

In equation (26), λ is the stretch ratio. In equation (25), α and β , which were taken from one of the in vitro human superficial nasal fascia specimens (n10js) reported in Zeng et al,¹⁰ are: $\alpha = 16.85$, $\beta = 1.99$. We chose this specimen, which was the softest of all four specimens of fascia reported by those researchers,¹⁰ to determine if our model equations could predict significant compression and shear in such an extreme case.

We also used the longitudinal stress-strain relation for incompressible material¹⁶ in our model. This relation is expressed by the following set of equations:

$$(27) \sigma = 2C_1C_2\left(\lambda^2 - \frac{1}{\lambda}\right)e^{C_2(I_1-3)}, \text{ with } \psi = 0, I_1 = \lambda^2 + \frac{2}{\lambda},$$

using $\lambda_1^2 = \lambda^2, \lambda_2^2 = \lambda_3^2 = \frac{1}{\lambda}$

We next used the theoretical stress given by equation (27) and the experimental stress given by equation (25) to calculate the values of C_1 and C_2 that would allow the theoretical and experimental curves of stress-stretch ratio to be as close to each other as possible (Figure 2). Our model minimized the sum of the squares of difference between the theoretical and experimental values of stress by using the least-square method¹⁹ directly on equations (25) and (27), in conjunction with a finite-difference method adapted from Newton's method for nonlinear equation systems.²⁰ The computed value of C_1 was 0.0327 MPa, and that of C_2 was 8.436 MPa.

Following the above procedure in conjunction with the available in vitro longitudinal stress-strain data from Wright and Rennels,¹¹ we determined the values of the elastic constant, C_1 , and the dimensionless constant, C_2 , for fascia lata and plantar fascia (Table 1). The mechanical constants for superficial nasal fascia were determined based on Zeng et al.¹⁰

Model Equations in the Laboratory Setting

We used our model equations to evaluate the deformations produced as a result of manual therapy in a subject's fascia lata, plantar fascia, and superficial nasal fascia. These fascia were subjected to normal pressure and shear forces (ie, without the longitudinal force). Fascia lata and plantar fascia are common sites for soft tissue osteopathic manipulative techniques in patients.²¹

The subject in our laboratory setting was the lead author of the present study (H.C.). Manual therapy was provided by

Jason DeFillipps, a rolfer who trained at the Rolf Institute in Boulder, Colo. Rolwing, which is also referred to as *structural integration* in osteopathic medicine, is a manual technique in which the practitioner is trained to observe both obvious movement of the skeleton and more subtle motion evidenced by slight muscle contraction visible through the overlying skin.^{1,22} Rolfers are not trained in diagnosis and treatment of specific conditions—as are osteopathic physicians—but rather in therapies to improve posture and general ease of function.^{1,22}

First, we conducted a laboratory test on the superficial nasal fascia of the subject to determine the amount of compression and stretch that is produced under the measured values of normal pressure and shear force. This test allowed us to compare the elastic properties of the subject's nasal fascia with that of the in vitro nasal fascia specimen reported by Zeng et al.¹⁰ For this test, the subject lay supine on a rigid platform on a force plate of the EquiTest computerized dynamic posturography apparatus (SmartEquitest System 2001; NeuroCom International Inc, Clackamas, Ore), which is capable of measuring the vertical ground reaction force and the shear force with a resolution of 0.89 N.

The therapist manipulated the nasal fascia of the subject with two fingers oriented caudally at a 30-degree angle to the surface of the skin just superior to the cartilaginous structure of the nose. Both normal and tangential pressure were applied with the rolwing technique (ie, structural integration).¹ This technique is generally regarded as the form of manual therapy that uses the greatest pressure.¹ The ground reaction and shear forces were collected with the EquiTest device for 20 seconds, sampled at a rate of 100 Hz, both before and during myofascial manipulation. Because we encountered technical problems with the initial synchronization in data collection for superficial nasal fascia, we did not use the data collected during the first 4 seconds for this tissue. In the case of fascia lata, however, we were able to use the data generated through the entire 20-second collection period.

Results

Measurements of Compression and Shear

The values at any time, t , during the 16-second collection period for change in ground reaction forces before and during myofascial manipulation of the subject's superficial nasal fascia are plotted in Figure 3A (applied normal force) and Figure 3B (applied shear force). The change in the measurements shown in Figure 3A and Figure 3B is the normal force and the tangential (ie, shear) force, respectively, applied by the manual therapist. These forces were converted into the normal pressure and the tangential stress by dividing the forces by the area of pressure application, which was 1.27 in² (8.18 cm²).

The predicted values of k_3 and k_1 (the compression and shear ratios, respectively) at any time, t , during the 16-second collection period for superficial nasal fascia were determined numerically by solving the set of nonlinear equations (22) and

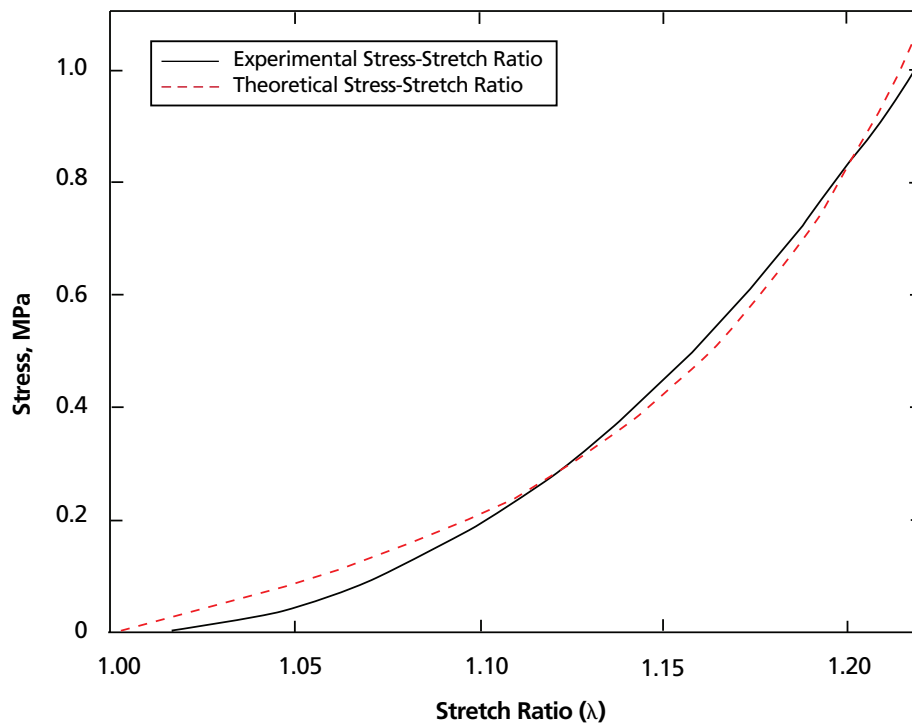


Figure 2. Experimental and theoretical stress-stretch ratio curves for superficial nasal fascia.

(23). These values are plotted in Figure 3C (k_3) and Figure 3D (k_1). The applied pressure, on average, was 52 kPa.

Figure 3A illustrates that a maximum applied compressive force of approximately 100 N occurs at the time of about $t = 7.25$ seconds. The force at this time must produce the maximum observed compression of the subject's superficial nasal fascia. This conclusion can be verified from the data in Figure 3C, which shows that a maximum compression of $k_3 = 0.91$ (ie, 9% compression) also occurs at about $t = 7.25$ seconds. A similar relation between the timing and amount of maximum applied shear force (Figure 3B) and maximum shear produced (Figure 3D) was also observed.

These data allowed us to compute the time history of compression and stretch of superficial nasal fascia produced during manual therapy. The resulting theoretical predictions based on our mathematical model are physiologically reasonable. Thus, as much as 9% compression and 6% shear can be achieved in superficial nasal fascia with forces in the range typically applied during manual therapies.

The same laboratory procedure and mathematical modeling used for the subject's superficial nasal fascia was also applied to the subject's fascia lata and plantar fascia, based on equations (22) and (23).

The plots of applied normal force and applied shear force for the subject's fascia lata during the 20-second data collection period are presented in Figure 4A (normal force) and Figure 4B

(shear force). The plots for values of the compression ratio (k_3) and shear ratio (k_1) for fascia lata are not presented because they were negligibly small under the applied loads. In the case of fascia lata, a predicted normal load of 9075 N (925 kg) and a tangential force of 4515 N (460 kg) are needed to produce even 1% compression and 1% shear. Such forces are far beyond the physiologic range of manual therapy.

Although the shear force applied to the subject's plantar fascia was measured using the EquiTest apparatus, it was not possible to measure the normal force on the plantar fascia using this device (ie, the normal force is parallel to the surface of the device's platform). For measuring the normal force, we

Table 1
Mechanical Constants for Fasciae,
Based on In Vitro Stress-Strain Data

Fascia Type	Mechanical Constant, MPa*	
	C_1	C_2
Fascia lata ¹¹	2.883	32.419
Plantar fascia ¹¹	0.931	61.775
Superficial nasal fascia ¹⁰	0.033	8.436

* C_1 is a constant analogous to modulus of elasticity; C_2 is a dimensionless constant.

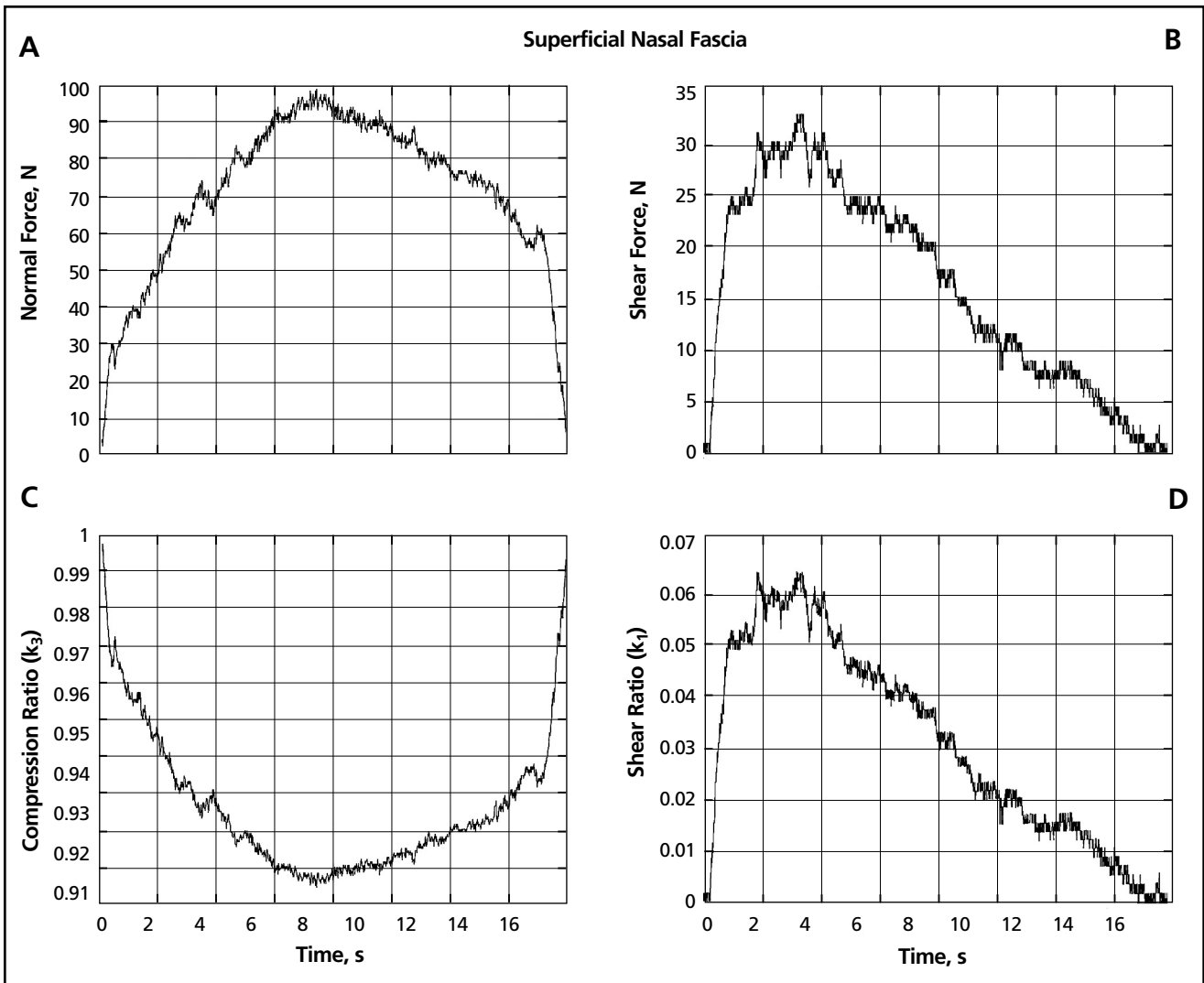


Figure 3. Measured forces and predicted force values during a 16-second myofascial release technique applied to superficial nasal fascia: (A) applied normal force, (B) applied shear force, (C) predicted values of compression ratio (k_3), and (D) predicted values of shear ratio (k_1).

Smaller values of the compression ratio mean more compression, consistent with the pattern of normal force. The pattern of shear ratio follows the pattern of shear force.

used the Xsensor pressure mapping system (X3 Lite Seat System, Version 4.2.5; XSENSOR Technology Corp, Calgary, Canada). This system can also be used to measure the maximal therapeutic pressure application to an area of fascia (Figure 5), a measurement that is useful to the manual therapist in patient treatment. The plots of normal and shear forces applied to the plantar fascia are presented in Figure 4C (normal force) and Figure 4D (shear force).

As with fascia lata, the plots for values of the compression ratio (k_3) and shear ratio (k_1) for plantar fascia are not presented because they were negligibly small under the applied loads. We found that, for plantar fascia, a normal load of 8359 N (852 kg) and a tangential force of 4158 N (424 kg) are needed to produce even 1% compression and 1% shear. These forces are far beyond the physiologic range of manual therapy,

as were the forces that were needed to produce compression and shear in fascia lata. Thus, we conclude that the dense tissues of fascia lata and plantar fascia both remain very stiff under compression and shear during manual therapy.

It was also observed, from equations (22) and (23), that for a specified value of compressive stress N and shear stress T , the values of k_3 (compression) and k_1 (shear) are not independent. If the values of k_3 and k_1 are specified, the values of compressive stress and shear stress depend on each other. The relation between these variables is given by the following:

$$N/T = \frac{k_3^2 - 1}{k_1 k_3}$$

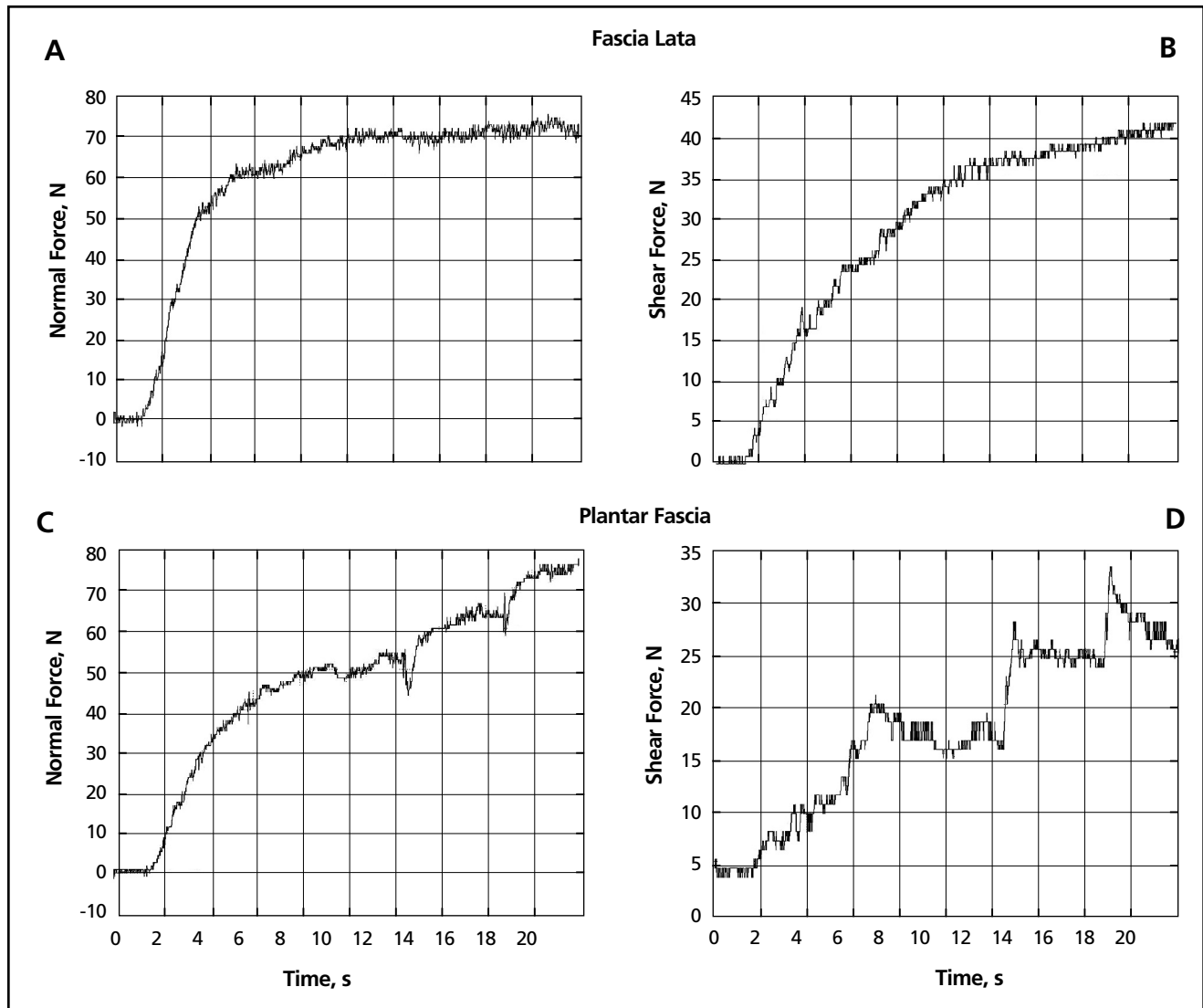


Figure 4. Measured forces during a 20-second myofascial release technique applied to fascia lata ([A] applied normal force, [B] applied

shear force) and plantar fascia ([C] applied normal force, [D] applied shear force).

Similarly, the relation between compressive stress and shear stress from equations (22) and (24) can also be established. Thus, the manual therapist cannot apply the forces arbitrarily if the fascia is to remain intact.

Comparison of Predicted Stresses for Plastic Deformation Under Longitudinal Force

We find from experimental measurements by Threlkeld⁷ of therapeutic pressure on fascia lata, which is plotted in Figure 5, that plastic deformation in the range of 3% to 4.13% elongation in the microfailure region of connective tissue occurs in the stress range of 788 N/cm² to 1997 N/cm². It is important to note that in Figure 5, 3% elongation can be observed at 4 mm displacement when microfailure begins, and 4.13% elongation is interpolated when microfailure ends, at 5.5 mm displacement.

We used experimental stress values (but not experimental

force values) in our model because there is a wide variation in the cross-sectional area of fasciae, and the thickness in the area of cross section (ie, width multiplied by thickness) has a negative correlation with subject age.²³ The experimental stress values used in our model were evaluated by dividing the force values (246 N-623 N) by the estimated area of cross section (0.312 cm²).²³

To compare our predicted stress range for the plastic deformation of 3% to 4.13%, based on our equation (24) in a three-dimensional setting and with an experimental stress range provided by Threlkeld,⁷ we calculated the longitudinal stress F for the two dense fasciae (fascia lata and plantar fascia) using the following values:

$$k_1 = 0 \text{ (no shear)}, k_3 = 1 \text{ (no compression)}, k_4 = 0.03\text{-}0.0413 \text{ (for extension)}$$

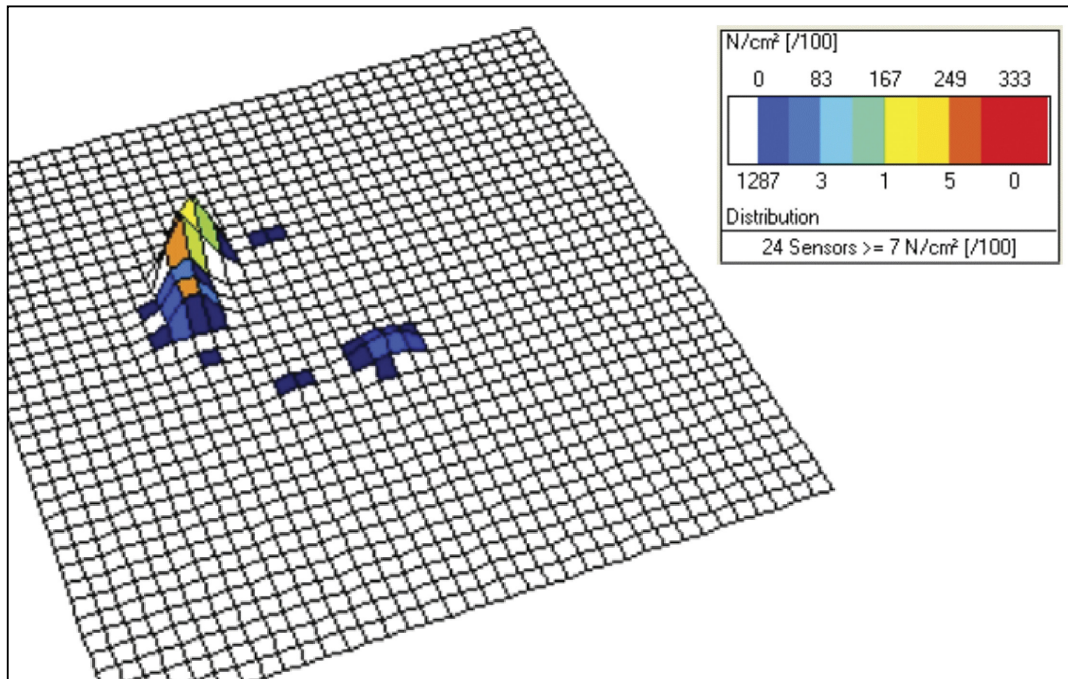


Figure 5. Plot of experimental measurements of maximal therapeutic pressure application (N/cm^2) on fascia lata,⁷ generated with the Xsensor pressure mapping

system (X3 Lite Seat System, Version 4.2.5; XSENSOR Technology Corp, Calgary, Canada).

The ranges of predicted stress values we found for plastic deformation of fascia lata and plantar fascia are provided in *Table 2*, with comparison to the known experimental fascial stress range reported by Threlkeld.⁷ Also in *Table 2* are the predicted values of compression and shear ratios. Predicted results for superficial nasal fascia are not included in *Table 2* because superficial nasal fascia is not dense fascia and, thus, should not be compared with known experimental stress ranges for dense fascia.

The differences between our predicted values for plastic deformation of fascia lata and plantar fascia and the experimental values for plastic deformation of general fascia⁷ can be attributed to the fact that mechanical properties of the fasciae of our subject (H.C.) may be different from those of the in vitro sample of connective tissue reported by Threlkeld.⁷ Moreover, Threlkeld⁷ obtained his experimental values for stress range by assuming a linear stress-strain relation, whereas our predictions are based on the actual nonlinear stress-strain relation observed in our volunteer subject.

We also note that for superficial nasal fascia, the predicted stresses for plastic deformation are very low (3.46–4.92 N/cm^2)—as would be expected because superficial nasal fascia consists of very soft tissues.

Comment

Our mathematical model of deformation of human fascia can also be used for fascia that is deformed by elongation only

($k_3 = 1, k_1 = 0$), compression only ($k_4 = k_1 = 0$), or shear only ($k_3 = 1, k_4 = 0$).

We can use the values of the mechanical parameters obtained in the present study to perform finite element analyses on the actual irregular shape of fasciae. As previously noted, the mathematical model we present in the current study is based on the assumption that fascia is an isotropic material. However, in some parts of the body, there are clear directional differences in fascial structural properties—differences that are often exploited by surgeons in planning skin incisions.²⁴ If fascia is anisotropic, then the elastic properties of anisotropic fascia in three dimensions must be determined in future calculations to obtain accurate predictions of tissue deformation under applied force.

We used available in vitro data for dense fasciae^{7,11} to evaluate the magnitude of forces required to produce specific deformations in these fasciae. We concluded that the magnitude of these evaluated forces is outside the physiologic range of manual therapy. This conclusion is supported by the findings of Sucher et al⁶ that in vitro manipulation of the carpal tunnel area on human cadavers leads to plastic deformation only if the manipulation is extremely forceful or lasts for several hours.

Ward²⁵ describes manual techniques central to osteopathic medicine (integrated neuromusculoskeletal release, myofascial release) that are designed to stretch and reflexively release restrictions in soft tissue. These techniques incor-

Table 2
Stress Ranges for Plastic Deformation of In Vitro Fasciae,
With Compression and Shear Ratios

Fascia Type	Stress Range, N/cm ²	Compression and Shear Ratio Under Stress
Fascia lata*	1275.00-1949.00	Negligibly small
Plantar fascia*	869.65-1454.00	Negligibly small
General Fascia†	788.00-1997.00	Data not provided

* Predicted stress range based on the authors' original calculations.
† Experimental stress range based on analysis by Threlkeld⁷ using Xsensor pressure mapping system (X3 Lite Seat System, Version 4.2.5; XSENSOR Technology Corp, Calgary, Canada).

porate fascial compression, shear, traction, and twist. Our results indicate that compression and shear alone, within the normal physiologic range, cannot directly deform the dense tissue of fascia lata and plantar fascia, but these forces can impact softer tissue, such as superficial nasal fascia.

Conclusions

We have developed a three-dimensional mathematical model for establishing the relationship between the mechanical forces and fascial deformations produced in manual therapy. The experimental results for the longitudinal stress-strain relation for fascia lata, plantar fascia, and superficial nasal fascia previously reported^{10,11} were compared with our original data. Because fascia is known to experience finite strain when subjected to longitudinal force,¹⁰ a finite deformation theory¹⁶ was used to predict the magnitude of the mechanical forces applied on the surface of fascia subjected to a specified finite deformation. Thus, with the help of the equations developed in the present study, the amount of deformation produced in fascia subjected to a known mechanical force can be determined. Conversely, if the amount of deformation is known, the magnitude of force needed to produce it can be determined.

The mathematical model described in the present study should be of great value to osteopathic physicians and other manual therapists, helping them determine the amount of force required to deform connective tissue to a given extent. In addition, we used our new model to determine changes in the amount of compression and shear produced with manual therapy over time. These calculations were made possible by using the EquiTest computerized dynamic posturography apparatus and the Xsensor pressure mapping system.

Our calculations reveal that the dense tissues of plantar fascia and fascia lata require very large forces—far outside the human physiologic range—to produce even 1% compression and 1% shear. However, softer tissues, such as superficial nasal fascia, deform under strong forces that may be at the upper bounds of physiologic limits. Although some manual therapists^{3,4} anecdotally report palpable tissue release in dense fasciae, such observations are probably not caused by deformations produced by compression or shear. Rather, these pal-

pable effects are more likely the result of reflexive changes in the tissue—or changes in twisting or extension forces in the tissue.²⁵

The mechanical forces generated by OMT and other forms of manual therapy may stimulate fascial mechanoreceptors, which may, in turn, trigger tonus changes in connected skeletal muscle fibers. These muscle tonus changes might then be felt by the practitioner.⁸ Alternatively, in vivo fascia may be able to respond to mechanostimulation with an altered tonus regulation of its own—myofibroblast-facilitated active tissue contractility.^{26,27} Such alternative explanations for fascial response to OMT and other manual therapies require further investigation.

Acknowledgments

We thank Jason DeFillipps, certified rolfer, for performing manual therapy in the present study.

References

- Rolf IP. Fascia—organ of support. In: Rolf IP. *Rolfing: Reestablishing the Natural Alignment and Structural Integration of the Human Body for Vitality and Well-Being*. Rochester, Vt: Healing Arts Press; 1989:37-44.
- Ward RC. Myofascial release concepts. In: Basmajian JV, Nyberg RE, eds. *Rational Manual Therapies*. Baltimore, Md: Williams & Wilkins; 1993:223-241.
- Smith J. The techniques of structural bodywork. *Structural Bodywork*. London, England: Churchill Livingstone; 2005.
- Stanborough M. *Direct Release Myofascial Technique: An Illustrated Guide for Practitioners*. London, England: Churchill Livingstone; 2004.
- Stecco L. *Fascial Manipulation for Musculoskeletal Pain*. Padova, Italy: Piccin Nuova Libreria; 2004.
- Sucher BM, Hinrichs RN, Welcher RL, Quiroz L-D, St Laurent BF, Morrison BJ. Manipulative treatment of carpal tunnel syndrome: biomechanical and osteopathic intervention to increase the length of the transverse carpal ligament: part 2. Effect of sex differences and manipulative "priming." *J Am Osteopath Assoc*. 2005;105:135-143. Available at: <http://www.jaoa.org/cgi/content/full/105/3/135>. Accessed July 29, 2008.
- Threlkeld AJ. The effects of manual therapy on connective tissues. *Phys Ther*. 1992;72:893-902. Available at: <http://www.ptjournal.org/cgi/reprint/72/12/893>. Accessed July 29, 2007.
- Schleip R. Fascial plasticity—a new neurobiological explanation: part 1. *J Bodywork Movement Ther*. 2003;7:11-19. Available at: <http://www.somatics.de/FascialPlasticity/Part1.pdf>. Accessed July 29, 2008.

(continued)

ORIGINAL CONTRIBUTION

9. Iatridis JC, Wu J, Yandow JA, Langevin HM. Subcutaneous tissue mechanical behavior is linear and viscoelastic under uniaxial tension. *Connect Tissue Res.* 2003;44:208-217.
10. Zeng YJ, Sun XP, Yang J, Wu WH, Xu XH, Yan YP. Mechanical properties of nasal fascia and periosteum. *Clin Biomech (Bristol, Avon).* 2003;18:760-764.
11. Wright DG, Rennels DC. A study of the elastic properties of plantar fascia. *J Bone Joint Surg Am.* 1964;46:482-492.
12. Keller TS, Colloca CJ, Béliveau JG. Force-deformation response of the lumbar spine: a sagittal plane model of posteroanterior manipulation and mobilization. *Clin Biomech (Bristol, Avon).* 2002;17:185-196.
13. Solinger AB. Theory of small vertebral motions: an analytic model compared to data. *Clin Biomech (Bristol, Avon).* 2000;15:87-94.
14. van Zoest GG, Gosselin G. Three-dimensionality of direct contact forces in chiropractic spinal manipulative therapy. *J Manipulative Physiol Ther.* 2003;26:549-556.
15. van Zoest GG, van den Berg HT, Holtkamp FC. Three-dimensionality of contact forces during clinical manual examination and treatment: a new measuring system. *Clin Biomech (Bristol, Avon).* 2002;17:719-722.
16. Green AE, Zerna W. *Theoretical Elasticity.* Oxford, England: Clarendon Press; 1968.
17. Demiray H. Stresses in ventricular wall. *J Appl Mech.* 1976;43:194-197.
18. Fung YC. *A First Course in Continuum Mechanics.* 3rd ed. Upper Saddle River, NJ: Prentice Hall; 1994:64-144.
19. Dahlquist G, Björck A. Approximation of functions. *Numerical Methods.* Mineola, NY: Dover Publications; 2003:81-136.
20. Gerald CF, Wheatley PO. Solving nonlinear equations. *Applied Numerical Analysis.* 6th ed. New York, NY: Addison Wesley Pub; 1999.
21. Ward RC, ed. *Foundations for Osteopathic Medicine.* Baltimore, Md: Williams and Wilkins; 1997:792-793.
22. Rolf Institute of Structural Integration Web site. Available at: <http://www.rolf.org/>. Accessed July 29, 2008.
23. Goh LA, Chhem RK, Wang SC, Chee T. Iliotibial band thickness: sonographic measurements in asymptomatic volunteers. *J Clin Ultrasound.* 2003;31:239-244.
24. Cerda E. Mechanics of scars. *J Biomech.* 2005;38:1598-1603.
25. Ward RC. Integrated neuromusculoskeletal release and myofascial release. *Foundations for Osteopathic Medicine.* 2nd ed. Philadelphia, Pa: Lippincott, Williams & Wilkins; 2003:931-965.
26. Schleip R, Klingler W, Lehmann-Horn F. Active fascial contractility: fascia may be able to contract in a smooth muscle-like manner and thereby influence musculoskeletal dynamics. *Med Hypotheses.* 2005;65:273-277.
27. Schleip R, Naylor IL, Ursu D, Melzer W, Zorn A, Wilke HJ, et al. Passive muscle stiffness may be influenced by active contractility of intramuscular connective tissue. *Med Hypotheses.* 2006;66:66-71.
-

Principles to an Osteopath means a perfect plan and specification to build in form a house, an engine, a man, a world, or anything for an object or purpose. To comprehend this engine of life or man which is so constructed with all conveniences for which it was made, it is necessary to constantly keep the plan and specification before the mind, and in the mind, to such a degree that there is no lack of knowledge of the bearings and uses of all parts.

Andrew Taylor Still, MD, DO
"Principles" from *Philosophy of Osteopathy* (1899)